JOURNAL OF AGRICULTURAL AND FOOD CHEMISTRY

Biotechnology and Biological Transformations

Biotechnological Production of Odor-active Methyl-Branched Aldehydes by a Novel #-Dioxygenase from *Crocosphaera subtropica*

Andreas Klaus Hammer, Florian Albrecht, Friederike Hahne, Paulina Jordan, Marco Alexander Fraatz, Jakob P. Ley, Torsten Geissler, Jens Schrader, Holger Zorn, and Markus Buchhaupt

J. Agric. Food Chem., **Just Accepted Manuscript** • DOI: 10.1021/acs.jafc.0c02035 • Publication Date (Web): 12 May 2020

is published by the American Chemical Society. 1155 Sixteenth Street N.W., Washington, DC 20036

Biotechnological Production of Odor-active Methyl-Branched Aldehydes by a Novel *α*-Dioxygenase from *Crocosphaera subtropica*

Andreas K. Hammer[†], Florian Albrecht[†], Friederike Hahne[†], Paulina Jordan[¥], Marco A. Fraatz[†,‡], Jakob Ley[§], Torsten Geissler[§], Jens Schrader[¥], Holger Zorn[†,‡,*], Markus Buchhaupt[¥]

[†]Justus Liebig University Giessen, Institute of Food Chemistry and Food Biotechnology, Heinrich-Buff-Ring 17, 35392 Giessen, Germany

[‡]Fraunhofer Institute for Molecular Biology and Applied Ecology, Winchester Str. 2, 35394 Giessen, Germany

[§]Symrise AG, Muehlenfeldstrasse 1, 37603 Holzminden, Germany

[¥]DECHEMA Research Institute, Industrial Biotechnology, Theodor-Heuss-Allee 25, 60486 Frankfurt am Main, Germany

ORCID

Andreas Klaus Hammer: 0000-0001-9226-1993

Florian Albrecht: 0000-0002-8140-5207

Friederike Hahne: 0000-0001-7731-5324

Marco Alexander Fraatz: 0000-0002-5028-9653

Jakob Ley: 0000-0001-9388-4260

Torsten Geißler: 0000-0001-5281-2324

Jens Schrader: 0000-0003-2235-6553

Holger Zorn: 0000-0002-8383-8196

Markus Buchhaupt: 0000-0003-2720-5973

* Corresponding author. Tel.: +49 (0) 641 99 34 900

E-mail address: holger.zorn@uni-giessen.de

Abstract

Due to their pleasant odor qualities and low odor thresholds, *iso*- and *anteiso*-fatty aldehydes represent promising candidates for applications in flavoring preparations. A novel cyanobacterial *α*-dioxygenase from *Crocosphaera subtropica* was heterologously expressed in *E. coli* and applied for the biotechnological production of C_{11} – C_{15} branched-chain fatty aldehydes. The enzyme has a sequence identity of less than 40% to the well investigated *α*-dioxygenase from rice. Contrary to the latter, it efficiently transformed short chained fatty acids. The kinetic parameters of the *α*-dioxygenase towards unbranched and *iso*-branched-chain substrates were studied by means of an oxygen depletion assay. The transformation products (C_{12}–C_{15} *iso*- and *anteiso*-aldehydes) were extensively characterized including their sensory properties. The aldehydes exhibited green-soapy, sweety odors with partial citrus-like, metallic, peppery, and savory-tallowy nuances. Moreover, the two C_{14} isomers showed particularly low odor threshold values of 0.2 and 0.3 ng/L air as determined by means of GC-olfactometry.

Keywords

methyl-branched aldehydes, flavoring substances, *α*-dioxygenase, *Crocosphaera subtropica* (former *Cyanothece sp.* ATCC 51142), odor threshold

Introduction

Various aldehydes are shaping the scent of flowers and the aroma of leaves, fruits, vegetables, and meat. The perceived odors greatly differ with the chemical structure (i.e. chain length, degree of unsaturation, and methyl branches), exhibiting for instance cucumber ((2*E*,6*Z*)-nona-2,6-dienal) or fatty, incense-like (2-methylundecanal) impressions, to itemize only two representatives.[1,2] 12-Methyltridecanal, a character impact compound of stewed beef, exhibits a low odor threshold[3,4] and is the most prominent representative of the class of branched-chain fatty aldehydes. Reports on the occurrence of *iso*- and *anteiso*-methyl-branched fatty aldehydes in food are rather scarce. C_8–C_{11} isomers were particularly detected in citrus essential oils and leaves of the curry tree *Bergera koenigii* L.,[5,6] while longer chained members of this class (C_{12}–C_{17}) have been mainly described in foods of animal origin like meat (especially of ruminants) and cheese.[3,7–9] Bacteria are well-known producers of branched-chain fatty acids,[10] and the aldehyde formation is presumed to be associated with the activity of microorganisms. Ruminal bacteria are discussed to produce branched-chain aldehydes, which are resorbed, incorporated in the ruminant plasmalogenes of muscles and afterwards released during stewing.[11]

Interestingly, not only bacteria, but also fungi like *Conidiobolus heterosporus* produce methyl-branched fatty acids to a large extent. Lipids of the latter fungus were successfully utilized in the biotechnological production of 12-methyltridecanal by means of a carboxylic acid reductase (CAR).[12] The need for costly cofactors (ATP, NADPH) as well as over-reduction to the alcohols are obstacles for the industrial application of CARs. These problems may be solved by cofactor recycling and the use of special *E. coli* strains with reduced alcohol dehydrogenase and aldo-keto reductase activities.[13–15]

43 *α*-Dioxygenases (*α*-DOX) represent an alternative enzymatic tool for aldehyde production,
44 which reduce carboxylic acids via a different reaction mechanism without the need of any
45 cofactors but molecular oxygen. Additionally, *E. coli* cells expressing *α*-DOX exhibit a lower
46 $NADH/NAD^+$ ratio, which makes the aldehyde production by whole cell catalysis easier
47 implementable.[16] On the other hand, there are drawbacks like a limited substrate spectrum:
48 due to a narrow substrate channel leading to the enzyme's active center, *α*-DOXs do solely
49 transform fatty acids, with a strong preference for long-chained representatives. Molecular
50 oxygen is added at the *α*-carbon, and the intermediate 2-hydroperoxy fatty acids either
51 spontaneously decarboxylate to release C_1-shortened aldehydes or are further enzymatically
52 converted to form the respective 2-hydroxy fatty acids (figure 1).[17–19] Fundamental knowledge
53 on this *α*-oxidation process was already obtained in the 1950s to 70s,[20–23] and many *α*-DOXs
54 have been discovered in various plants since then.[19]
55 However, this is the first report on a bacterial *α*-DOX, originating from the cyanobacterium
56 *Crocosphaera subtropica* (former *Cyanothece sp.* ATCC 51142), which was found by alignment
57 of sequences encoding plant *α*-DOX enzymes with bacterial sequences of moderate similarity.
58 Its capability for the conversion of saturated fatty acids as well as the acceptance of methyl-
59 branched substrates was tested. Reaction optima were determined and kinetic parameters
60 for unbranched and branched-chain substrates were compared. Eight *iso*- and *anteiso*-methyl-
61 branched aldehydes (C_{12}–C_{15}) were produced on a semi-preparative scale, and their odor
62 properties were investigated.
63
64

Materials and methods

Chemicals.

Myristic acid (99%), pentadecanoic (99%), and undecanoic acid (99%) were purchased from Acros Organics (Geel, Belgium), acetonitrile (99.95%) from Actu-All Chemicals (Randmeer, Netherlands). Coomassie Brilliant Blue (CBB) R250 was supplied by AppliChem (Darmstadt, Germany), diethyl ether (99.5%) by BCH Bruehl Chemikalien Handel (Bruehl, Germany). Formic acid (98%) was obtained from Bernd Kraft (Duisburg, Germany). Chloroform-*d* (99.8 atom% D, with 0.03 vol% TMS, stabilized with Ag), dimethyl sulfoxide (DMSO, 99.5%), disodium hydrogen phosphate (99.5%), glycine (99%), imidazole (99%), Luria-Bertani (LB) agar and medium, 2-[4-(2,4,4-trimethylpentan-2-yl)phenoxy]ethanol (Triton X-100), tris(hydroxymethyl)-aminomethane (TRIS), and polysorbate (Tween® 20) were purchased from Carl Roth (Karlsruhe, Germany). *n*-Hexane (97%) was obtained from Honeywell (Seelze, Germany). 10-Methyldodecanoic acid (racemic mixture, 98%) and 11-methyldodecanoic acid (98%) were purchased from Larodan (Solna, Sweden), silica gel 60 from Macherey-Nagel (Düren, Germany), isopropyl-β-D-thiogalactopyranoside (IPTG) and kanamycin sulfate (Ph. Eur.) from Serva (Heidelberg, Germany). Tridecanoic acid (99%) was purchased from Sigma-Aldrich (Taufkirchen, Germany). Symrise (Holzminden, Germany) provided 11-methyl- and 12-methyltridecanoic acid, 12-methyl- and 13-methyltetradecanoic acid, as well as 13-methyl- and 14-methylpentadecanoic acid (98% each, anteiso-compounds were racemic mixtures). *n*-Pentane (99%) and potassium dihydrogenphosphate (99.5%) were supplied by Th. Geyer (Renningen, Germany). Hydrogen (5.0) and helium (5.0) were purchased from Praxair (Düsseldorf, Germany) and nitrogen (5.0) from Air Liquide (Düsseldorf, Germany). All numbers given in parentheses represent the minimum purity.

E. coli strains, vectors, and primers.

E. coli strain 10*β* was purchased from New England BioLabs (Frankfurt, Germany), strain BL21(DE3) and plasmid pET-28a from Merck (Darmstadt, Germany). A DNA fragment encoding a potential *α*-dioxygenase enzyme (GenBank entry ACB53655.1) from *Crocosphaera subtropica* (former *Cyanothece sp.* ATCC 51142[24]) with codon usage optimized for expression in *E. coli* was synthesized and transferred into pET-28a between *NcoI* and *XhoI* (pET-28a-*Csα*-DOX) by GeneArt (Regensburg, Germany). A construct allowing the expression of a C-terminal His-tagged *α*-DOX (pET-28a-*Csα*-DOX_C-His) was obtained by deletion of the stop codon via FastCloning.[25] Therefore, about 100 ng plasmid template DNA were amplified by means of polymerase chain reaction (PCR). The PCR cycling parameters were 98 °C (2 min), [98 °C (30 s), 68 °C (30 s), 72 °C (3 min)] x 30 cycles, 72 °C (15 min), and 8 °C infinite with 0.5 U phusion polymerase, High Fidelity buffer (both New England BioLabs), 0.2 mM dNTPs (Thermo Fisher), and 0.5 µM primers (5‘-TCG TGT TCC GAG CCT CGA GCA CCA CC-3’ (forward) and 5‘-GGT GGT GCT CGA GGC TCG GAA CAC GA-3‘ (reverse) by Biomers, Ulm, Germany). After *DpnI*-digestion (Thermo Fisher, Darmstadt, Germany) according to the manufacturer’s protocol, target plasmids were transformed in *E. coli* 10*β* for replication. Plasmid isolation (NucleoSpin® Plasmid kit, Macherey-Nagel) and sequencing (Microsynth Seqlab, Goettingen, Germany) as well as western blot of expressed *α*-DOX were carried out for control purposes.

Heterologous protein expression.

BL21(DE3)+pET-28a-*Csα*-DOX, BL21(DE3)+pET-28a-*Csα*-DOX_C-His, and BL21(DE3)+pET-28a cells were grown in LB medium (50 µg/mL kanamycin) at 37 °C in baffled shake flasks (180 rpm). At an OD_{600} of 0.6–0.8, expression of *α*-DOX was induced by addition

of 0.5 mM IPTG. The cultures were incubated for additional 16 h at 21 °C. The cells were harvested by centrifugation (3724*g*, 15 min, 4 °C) and frozen at −20 °C.

α-DOX expression was checked via sodium dodecyl sulfate−polyacrylamide gel electrophoresis (SDS−PAGE) according to Laemmli[26] (4% stacking, 12% resolving polyacrylamide gels, CBB R250 staining) and, in case of His-tagged *α*-DOX, by western blot. Towbin buffer (25 mM TRIS, 192 mM glycine, 5% (v/v) methanol)[27] was used for protein transfer from the SDS-PAGE gel onto a polyvinylidene fluoride membrane (Carl Roth, Karlsruhe, Germany, pore size 0.45 µm) by means of a Peqlab (Erlangen, Germany) PerfectBlue™ Tank Electro Blotter Web™ S (1000 mA, 75 min). The membrane was subsequently blocked over night at 4 °C with 5% milk powder solution in TBST buffer (50 mM TRIS (pH 7.5), 150 mM NaCl, 0.1% Tween® 20) and incubated with anti-His horseradish peroxidase (Carl Roth, Karlsruhe, Germany) for 2 h at room temperature (RT). The blot was developed with Opti-4CN™ substrate kit (Bio-Rad Laboratories) according to the manufacturer's instruction for 30 min at RT.

Substrate screening.

Cell pellets were washed with ½ culture volume of 200 mM phosphate buffer (pH 7.5) and resuspended in 1/50 culture volume of 50 mM phosphate buffer (pH 7.5). The cell suspensions were incubated for one hour on ice with lysozyme (100 µg/mL), followed by cell disruption for 4 min on ice using a Branson W 250 D digital sonifier (microtip diameter 5 mm, amplitude 10%, 240 pulses of 1 s followed by a pause of 3 s). Afterwards, the lysates were centrifuged (22,000*g*, 10 min, 4 °C) and the supernatant was used for the substrate screening after adjusting protein concentrations according to bicinchoninic acid method.[28]

An optical oxygen sensor (NTH-PSt1-L2.5-TS-NS40/1.2-NOP and OxyView TX3v602 program, PreSens, Regensburg, Germany) was applied for measurements of oxygen consumption

during α-DOX reaction (figure 1): Enzymatic conversions were monitored (5 s measuring interval) at room temperature in the cavities of a microtiter plate, equipped with a 4 mm stir bar (200 rpm). The total volume of the reaction mixture was 200 µL, containing 50 mM phosphate buffer (pH 7.5, 1% Triton X-100) and protein lysates (1.25 µg/µL). Substrate, dissolved in DMSO, was added to a final concentration of 1 mM to start the measurements. By measuring blanks with added DMSO but without substrate, the background oxygen consumption of the crude extracts was taken into account.

Purification of α-DOX.

20 to 25% (m/v, cell wet weight) suspensions of *E. coli* cells containing His-tagged α-DOX in disruption buffer (50 mM phosphate buffer (pH 7.5), 20 mM imidazole, 1% (v/v) Triton X-100) were disrupted on ice with a sonifier MS72 (Bandelin Electronic, Berlin, Germany) three times for 30 s each (amplitude 10%, cyclus 3) with 30 s breaks. The lysates were centrifuged (3,724*g*, 15 min, 4 °C), and the supernatants were used for further purification. The disruption procedure was repeated three times.

The purification of α-DOX was performed by means of Protino® nickel-nitrilotriacetic acid agarose (Ni-NTA, Macherey-Nagel) using the gravity-flow purification protocol according to the manufacturer's instructions. The enzyme was eluted with 50 mM phosphate buffer (pH 7.5) containing 250 mM imidazole, concentrated using 50 kDa centrifugal filters (Merck Millipore, Tullagreen, Ireland, 3,724*g*, 4 °C), and washed with 10 mL of 50 mM phosphate buffer (pH 7.5). The buffer was substituted by 50 mM phosphate buffer (pH 7.5) following the gravity protocol of Sephadex™ G-25 M PD-10 desalting columns (GE Healthcare, Little Chalfont, UK). The entire purification procedure was carried out at 4 °C. SDS–PAGE was applied for purity control. The concentration of α-DOX was determined photometrically at a

160 wavelength of 280 nm with a calculated extinction coefficient of ε = 96,433 1/M per cm,
161 deduced from the amino acid sequence by the ProtParam tool of ExPASy (Swiss Institute of
162 Bioinformatics, Lausanne Switzerland)[29].
163
164 Determination of salt-, pH-, and temperature-optima.
165 The influence of phosphate buffers of several concentrations (50, 100, 200, 400 mM),
166 pH-values (6, 7, 7.5, 8, 9), additives (NaCl, DMSO, Triton X-100), and temperatures (20, 25, 30,
167 35, 40 °C) on enzyme activity was examined.
168 The influence of buffer concentrations, pH-values, and addition of NaCl (50 mM) and of DMSO
169 (2.5%, v/v) was tested in 20 mL vials with a total reaction volume of 4 mL. The substrates
170 (undecanoic, tridecanoic, and pentadecanoic acid, 5 mM each) were dispersed for 5 min in a
171 Sonorex Super RK 510 H ultrasonic bath (Bandelin Electronic) in the respective reaction buffer
172 prior to the addition of purified α-DOX (10 µg/mL). Samples were mixed by means of rotary
173 incubator (Stuart, Stone, UK, 40 rpm, mixing angle 90°) for 1 h, immediately cooled on ice, and
174 200 µL of 4 M HCl were added. Prior to analysis, samples of different buffer compositions were
175 filled up to 8 mL and thereby adjusted to identical buffer, salt, and DMSO concentrations.
176 Product formation was investigated by means of headspace–solid phase microextraction–gas
177 chromatography–mass spectrometry (HS–SPME–GC–MS). The samples were incubated for
178 10 min (60 °C and 250 rpm agitation rate) by means of an MPS 2XL multipurpose sampler
179 (GERSTEL, Mülheim an der Ruhr, Germany), while the SPME fiber (PDMS/DVB, 1 cm x 65 µm,
180 Merck, Darmstadt, Germany) was baked out for 5 min (250 °C) in the needle heater station of
181 the autosampler. The samples were subsequently extracted for 30 min (same conditions as
182 for incubation). The analytes were desorbed in the inlet of the GC system (Merck SPME liner,
183 0.75 mm i.d.) at 250 °C for 90 s, and the fiber was reconditioned afterwards in the needle

heater station (10 min, 250 °C). The gas chromatography system used was an Agilent (Waldbronn, Germany) 7890A gas chromatograph, equipped with an Agilent VF-WAXms column (30 m × 0.25 mm; 0.25 µm film thickness; temperature program, 40 °C (3 min) at 5 °C/min to 240 °C (12 min); carrier gas, helium (1.56 mL/min, constant)) and a split/splitless (S/SL) inlet (250 °C). Analytes were detected by means of an Agilent 7000B triple quadrupole detector (ionization energy, 70 eV; ion source, 230 °C; quadrupoles, 150 °C; transfer line, 250 °C; scan in q1, *m/z* 33−300; helium quench gas (2.25 mL/min); and nitrogen collision gas (1.5 mL/min)).

Additionally, the influence of additives such as of NaCl (50 mM) and Triton X-100 (0.1, 0.5, and 1.0%, v/v) was tested on 300 µL scale with tridecanoic acid as substrate (5 µM) by means of an oxygen depletion assay.

Enzyme kinetic parameters.

An oxygen depletion assay was applied for determination of kinetic parameters. Oxygen consumption was analyzed every 10 s at 25 ± 2 °C. 285 µL of reaction buffer (200 mM phosphate buffer (pH 7.5), 50 mM NaCl, 1% (v/v) Triton X-100) were mixed (250 rpm) with 7.5 µL isolated α-DOX (stored over night at 4 °C, stock concentration 400 µg/mL), and 7.5 µL substrate dissolved in DMSO (stock concentrations ranging from 62.5 to 8,000 µM). Samples without enzymes, without substrate, and with denatured α-DOX (95 °C, 10 min) served as negative controls.

Michaelis-Menten kinetics with K_m, v_{max}, and k_{cat} for the substrates myristic and 13-methyltetradecanoic acid were calculated using OriginPro version 2020 (OriginLab Corporation, Northampton, MA).

Semi-preparative biotransformation experiments.

Several *iso*- and *anteiso*-methyl-branched fatty acids (figure 2) were used for biotransformation experiments on semi-preparative scale with purified *α*-DOX. Specific enzyme activity was determined by the oxygen depletion assay in reaction buffer (200 mM phosphate (pH 7.5), 50 mM NaCl) with 13-methyltetradecanoic acid (5 µM in reaction mixture). 0.25 U were applied for the transformation of 50 µmol substrate. Enzymatic conversions were carried out in the latter buffer on 4 mL scale by the method described under "Determination of salt-, pH-, and temperature-optima" at 25 °C.

Product isolation and identification.

Biotransformation broths were extracted 3 times with *n*-pentane/diethyl ether (1:1.12, v/v), and the combined extracts were dried over sodium sulfate. Aliquots were analyzed by means of gas chromatography–mass spectrometry (GC–MS) for the purpose of product yield estimation by calculating the relative peak shares of educts and products. The respective unbranched analogs were used for calculation of response factors. The extracts were concentrated using a Vigreux column (water bath temperature 43 °C) and subsequently purified by means of column chromatography (silica gel 60) with *n*-pentane/diethyl ether (95:5, v/v) as eluent. Structures were elucidated by atmospheric pressure chemical ionization–time of flight–mass spectrometry (APCI–TOF–MS), GC–MS, and nuclear magnetic resonance (NMR).

Accurate masses were obtained by means of ABSciex (Darmstadt, Germany) TripleTOF 5600+ system by direct infusion (100 µL/min) of the isolated products dissolved in *n*-hexane (10 µg/mL). Ionization was accomplished in APCI positive mode (ion spray voltage, 5500 V; ion spray temperature, 400 °C; nebulizer gas, 15 psi; auxiliary gas, 30 psi; curtain gas, 25 psi). The

mass detector was calibrated using a sodium formate solution (30 µL/min) in ESI positive mode (differing from above: auxiliary gas, 15 psi; ion spray temperature, ambient temperature).[30] Data analysis was performed using Analyst TF 1.7.1 and PeakView 2.2 software (ABSciex).

NMR experiments (^{1}H-NMR, ^{13}C-NMR, DEPT135, ^{1}H, ^{1}H correlation spectroscopy (COSY), and heteronuclear single-quantum correlation (HSQC)) with $CDCl_3$ as solvent were carried out on a Bruker (Rheinstetten, Germany) Avance II 400 MHz, Bruker Avance III 400 MHz HD, and Avance III 600 MHz at ambient temperature.

Sensory evaluation of methyl-branched aldehydes.

Odor qualities were determined by sniffing at the isolated substances as well as by means of GC–FID–O. For the latter, an Agilent 7890A GC equipped with an Agilent G4513A autosampler (sample volume 1 µL, cool on column injection (40 °C, track oven modus)) and an Agilent VF-WAXms column (30 m x 0.32 mm, 0.25 µm film thickness; temperature program, 40 °C (3 min) at 5 °C/min to 180 °C (0 min) and at 30 °C/min to 240 °C (12 min); carrier gas, hydrogen (3.5 mL/min, constant)) was applied. The gas flow was split 1:1 by a GERSTEL µFlowManager Splitter to a flame ionization detector (FID (250 °C); hydrogen, 40 mL/min; air, 400 mL/min; nitrogen, 25 mL/min) and a GERSTEL ODP3 (transfer line, 250 °C; mixing chamber, 150 °C; make up gas, nitrogen). Three trained panelists were asked to freely choose attributes.

Statistics.

Determination of salt-, pH-, and temperature-optima of *Csα*-DOX were performed in triplicate. The substrate spectrum was screened and kinetic parameters were calculated in

biological independent triplicates. The odor qualities of pure substances were evaluated by a panel of 6 trained persons (3 females and 3 males, 23 to 28 years of age), whereas GC–FID–O was evaluated five times by a panel of 3 trained persons (2 females, 1 male, 27 to 32 years of age). All panelists were weekly trained for the purpose of describing odor qualities.

Results and discussion

Expression, substrate screening and purification of *Csα*-DOX.

The *α*-DOXs from *Crocosphaera subtropica* (*Csα*-DOX) was successfully expressed in *E. coli* exhibiting a molecular mass of ~ 70 kDa in SDS–PAGE analysis (figure 3), in line with the calculated theoretical mass of 69.9 kDa. Western blot with an anti-His-horseradish peroxidase (cf. Supporting Information, figure S1) as well as DNA sequencing revealed a correct cloning procedure. During the screening of the various substrates, the expected oxygen depletion was observed (figure 4).

So far, only *α*-DOXs originating from plants like *Arabidopsis*,[31] tobacco,[31] pea,[32] or rice[33] have been described and characterized. This is the first report of an analogous enzyme originating from bacteria showing a sequence identity of 39% to the enzyme from rice (*Oryza sativa)*. Alignments of the helices 2, 6, 8 and 17 of the bacterial protein sequence and three plant *α*-DOX sequences showed that conserved regions shared by all members of the *α*-DOX protein family[18] are also contained in the *C. subtropica* protein (Supporting Information, figure S2). Especially three amino acids, which were shown to be indispensable for activity of the *O. sativa* enzyme (His-311, Tyr-379 and Arg-559), are present in the bacterial enzyme. The novel *Csα*-DOX was surprisingly shown to convert saturated fatty acids of a broad range of chain

lengths, with a maximum activity for lauric acid (figure 4). These findings are strikingly different from those of *Osα*-DOX from *O. sativa*, the probably most widely applied *α*-DOX. *Osα*-DOX has been reported in the literature to transform fatty acids with a minimum chain length of C_{10}.[16,18,34] Additionally, we observed an extremely weak activity towards hexanoic and octanoic acid of *Osα*-DOX in this study (cf. Supporting Information, figure S4). The novel enzyme from *C. subtropica* clearly outperformed the rice enzyme in the conversion of fatty acids with less than 16 carbon atoms. In general, the conversion of shorter chained substrates than C_{14} (in particular C_{12}) has been investigated only for a few other *α*-DOXs so far, and their activities were found to be low.[19,20,22] Lauric acid was also converted by a pea-*α*-DOX, but no comparative substrate spectrum was recorded in this study.[32]

To the best of our knowledge, methyl-branched substrates have not been investigated as substrates for any *α*-DOX so far. For detailed kinetic studies, the enzyme was purified to electrophoretic homogeneity (figure 3). Comparison of the activities of *α*-DOX variants with and without His-tag showed no negative influence of the C-terminal His-tag on the enzyme activity (cf. Supporting Information S5).

Determination of salt-, pH-, and temperature-optima.

The Thermofluor assay according to Boivin *et al.*[35] was applied for stability screening of the enzyme in different buffers. The results (data not shown) were used for a preselection of the conditions studied in detail as described below.

Although no common optimum was observed for all substrates, use of a 200 mM phosphate buffer with a pH value of 7.5 and 50 mM NaCl at a temperature of 25 °C yielded high overall conversion rates. Apart from the comparatively high ion concentration, this finding is in accordance with buffers typically used for *α*-DOX transformation assays.[18,22,31–34,36–38] The

origin of *Csα*-DOX from the marine cyanobacterium *C. subtropica*[24] may well explain the enzyme's preference for high salt concentrations.

DMSO has been reported as a performance-enhancing co-solvent,[39] but it had no influence on conversion rates of *Csα*-DOX. However, the addition of Triton X-100 doubled the relative enzyme activity when used in concentrations of 1% (v/v). Triton X-100 and further emulsifiers have also been employed for other *α*-DOX catalyzed bioconversions.[33,34,40,41] As Triton X-100 significantly impeded the extraction of the aldehydes from the reaction buffer, it was solely applied in the determination of enzyme kinetic parameters, but not for semi-preparative biotransformation experiments.

Enzyme kinetic parameters.

To evaluate the influence of methyl-branches close the substrates' *ω*-terminus on the enzymatic activity, kinetic parameters were determined for tetradecanoic acid and 13-methyltetradecanoic acid as substrate by means of the oxygen depletion assay (table 1, Supporting Information, figure S6). For other *α*-DOXs, only the impact of the chain length and of the presence of double bonds (number and position) has been investigated so far.[18,19,34,37] K_m and k_{cat} values for both substrates were comparable to those of other *α*-DOXs.[17,18,22,32,36–38]

The comparison of the catalytic efficiencies (k_{cat}/K_m) for both substrates (table 1) clearly demonstrated the absence of a substrate preference. These results support the current model for substrate binding: *α*-DOXs exhibit a channel leading to their active side. This channel interacts with the substrate's first seven carbon atoms, which is supposed to be of high importance for catalysis. Especially steric deviations in this substrate region are discussed to influence binding and therefore conversion rates dramatically.[17,18,42] As already shown in

literature, this channel seems to be responsible for the low acceptance of unsaturated fatty acids with double bonds within the first seven carbon atoms. The effect increased when substrates with double bonds closer to the carboxylic group were examined.[18,37]

Semi-preparative biotransformation experiments and identification of reaction products.

The intensely perceivable odor of biotransformation broths indicated successful bioconversions. Depending on the respective substrate, the product yields ranged from 20 – 61 mol%. After purification of the products, structure elucidation was performed by means of GC-MS, high resolution mass spectrometry, and NMR analyses.

NMR, GC–MS, and HRMS data of 9-methylundecanal.

^{1}H NMR ($CDCl_3$, 400 MHz): δ 9.77 (1 H, t, *J* = 2.0 Hz), 2.42 (2 H, td, *J* = 1.5 and 7.0 Hz), 1.63 (2 H, p, *J* = 7.0 Hz), 1.11–1.39 (13 H, m), 0.85 (3 H, t, *J* = 7.0 Hz), 0.84 (3 H, d, *J* = 6.5 Hz). ^{13}C NMR ($CDCl_3$, 100 MHz): δ 203.0, 43.9, 36.6, 34.4, 29.8, 29.5, 29.4, 29.2, 27.0, 22.1, 19.2, 11.4. GC-MS (EI, 70 eV): 96 (50), 95 (84), 82 (51), 81 (84), 70 (84), 69 (70), 67 (51), 57 (100), 55 (65), 41 (59). HRMS (APCI–TOF): 185.18926 Da, –4.0 ppm deviation from theoretical mass ($C_{12}H_{25}O^+$).

NMR, GC–MS, and HRMS data of 10-methylundecanal.

^{1}H NMR ($CDCl_3$, 400 MHz): δ 9.77 (1 H, t, *J* = 2.0 Hz), 2.42 (2 H, td, *J* = 2.0 and 7.5 Hz), 1.64 (2 H, p, *J* = 7.5 Hz), 1.50 (1 H, n, *J* = 6.5 Hz), 1.22–1.35 (10 H, m), 1.16 (2 H, m), 0.86 (6 H, d, *J* = 6.5 Hz). ^{13}C NMR ($CDCl_3$, 100 MHz): δ 203.0, 44.0, 39.0, 29.9, 29.5, 29.4, 29.2, 28.0, 27.4, 22.7, 22.7, 22.1. GC-MS (EI, 70 eV): 95 (53), 81 (52), 82 (84), 69 (59), 67 (45), 57 (100), 56 (60), 55 (58), 43 (70), 41 (56). HRMS (APCI–TOF): 185.18993 Da, –0.3 ppm deviation from theoretical mass ($C_{12}H_{25}O^+$).

NMR, GC–MS, and HRMS data of 10-methyldodecanal.

^{1}H NMR ($CDCl_3$, 600 MHz): δ 9.77 (1 H, t, *J* = 2.0 Hz), 2.42 (2 H, td, *J* = 2.0 and 7.5 Hz), 1.63 (2 H, p, *J* = 7.0 Hz), 1.04–1.35 (15 H, m), 0.85 (3 H, t, *J* = 7.0 Hz), 0.84 (3 H, d, *J* = 6.0 Hz). ^{13}C NMR ($CDCl_3$, 100 MHz): δ 203.0, 44.0, 36.6, 34.4, 29.9, 29.5, 29.5, 29.4, 29.2, 27.1, 22.1, 19.2, 11.4. GC-MS (EI, 70 eV): 95 (100), 82 (65), 83 (57), 81 (64), 71 (51), 70 (86), 69 (59), 57 (96), 55 (66), 41 (57). HRMS (APCI–TOF): 199.20511 Da, –2.7 ppm deviation from theoretical mass ($C_{13}H_{27}O^+$).

NMR, GC–MS, and HRMS data of 11-methyldodecanal.

^{1}H NMR ($CDCl_3$, 600 MHz): δ 9.77 (1 H, t, *J* = 2.0 Hz), 2.42 (2 H, td, *J* = 1.5 and 7.5 Hz), 1.63 (2 H, p, *J* = 7.0 Hz), 1.51 (1 H, n, *J* = 6.5 Hz), 1.20–1.35 (12 H, m), 1.15 (2 H, m), 0.86 (6 H, d, *J* = 6.5 Hz). ^{13}C NMR ($CDCl_3$, 100 MHz): δ 203.0, 44.0, 39.1, 29.9, 29.6, 29.5, 29.4, 29.2, 28.0, 27.4, 22.7, 22.7, 22.1. GC-MS (EI, 70 eV): 96 (62), 95 (59), 82 (89), 81 (56), 69 (62), 57 (100), 56 (54), 55 (58), 43 (68), 41 (51). HRMS (APCI–TOF): 199.20578 Da, 0.7 ppm deviation from theoretical mass ($C_{13}H_{27}O^+$).

NMR, GC–MS, and HRMS data of 11-methyltridecanal.

^{1}H NMR ($CDCl_3$, 600 MHz): δ 9.77 (1 H, t, *J* = 2.0 Hz), 2.42 (2 H, td, *J* = 2.0 and 7.5 Hz), 1.63 (2 H, p, *J* = 7.5 Hz), 1.10–1.32 (17 H, m), 0.85 (3 H, t, *J* = 7.0 Hz), 0.84 (3 H, d, *J* = 6.0 Hz).^{13}C NMR ($CDCl_3$, 100 MHz): δ 203.0, 44.0, 36.6, 34.4, 30.0, 29.6, 29.5, 29.5, 29.4, 29.2, 27.1, 22.1, 19.2, 11.4. GC-MS (EI, 70 eV): 109 (62), 96 (63), 95 (89), 83 (77), 82 (73), 81 (69), 70 (92), 57 (100), 55 (74), 41 (57). HRMS (APCI–TOF): 213.22081 Da, –2.3 ppm deviation from theoretical mass ($C_{14}H_{29}O^+$).

NMR, GC–MS, and HRMS data of 12-methyltridecanal.

^{1}H NMR ($CDCl_3$, 600 MHz): δ 9.76 (1 H, t, *J* = 1.5 Hz), 2.42 (2 H, td, *J* = 1.5 and 7.5 Hz), 1.63 (2 H, p, *J* = 7.0 Hz), 1.51 (1 H, n, *J* = 6.5 Hz), 1.23–1.34 (14 H, m), 1.13 (2 H, m), 0.86 (6 H, d, *J* = 6.5 Hz). ^{13}C NMR ($CDCl_3$, 100 MHz): δ 203.0, 43.9, 39.1, 29.9, 29.7, 29.6, 29.4, 29.4, 29.2,

28.0, 27.4, 22.7, 22.7, 22.1. GC-MS (EI, 70 eV): 96 (63), 95 (61), 82 (100), 81 (56), 69 (63), 57 (100), 56 (54), 55 (59), 43 (70), 41 (51). HRMS (APCI–TOF): 213.22140 Da, 0.5 ppm deviation from theoretical mass ($C_{14}H_{29}O^+$).

NMR, GC–MS, and HRMS data of 12-methyltetradecanal.

^{1}H NMR ($CDCl_3$, 600 MHz): δ 9.77 (1 H, t, *J* = 2.0 Hz), 2.42 (2 H, td, *J* = 2.0 and 7.5 Hz), 1.63 (2 H, p, *J* = 7.0 Hz), 1.08–1.33 (19 H, m), 0.85 (3 H, t, *J* = 7.0 Hz), 0.84 (3 H, d, *J* = 6.0 Hz). ^{13}C NMR ($CDCl_3$, 100 MHz): δ 203.0, 44.0, 36.7, 34.4, 30.0, 29.7, 29.6, 29.5, 29.5, 29.4, 29.2, 27.1, 22.1, 19.2, 11.4. GC-MS (EI, 70 eV): 97 (63), 96 (64), 95 (88), 83 (69), 82 (80), 81 (69), 71 (62), 70 (93), 57 (100), 55 (74). HRMS (APCI–TOF): 227.23723 Da, 1.3 ppm deviation from theoretical mass ($C_{15}H_{31}O^+$).

NMR, GC–MS, and HRMS data of 13-methyltetradecanal.

^{1}H NMR ($CDCl_3$, 400 MHz): δ 9.77 (1 H, t, *J* = 2.0 Hz), 2.42 (2 H, td, *J* = 2.0 and 7.5 Hz), 1.63 (2 H, p, *J* = 7.0 Hz), 1.51 (1 H, n, *J* = 6.5 Hz), 1.20–1.30 (16 H, m), 1.15 (2 H, m), 0.86 (6 H, d, *J* = 6.5 Hz). ^{13}C NMR ($CDCl_3$, 100 MHz): δ 203.0, 44.0, 39.1, 30.0, 29.7, 29.7, 29.6, 29.4, 29.4, 29.2, 28.0, 27.4, 22.7, 22.7, 22.1. GC-MS (EI, 70 eV): 96 (71), 95 (58), 83 (53), 82 (100), 81 (53), 69 (60), 57 (97), 56 (49), 55 (58), 43 (67). HRMS (APCI–TOF): 227.23713 Da, 0.8 ppm deviation from theoretical mass ($C_{15}H_{31}O^+$). The structures of the formed aldehydes are depicted in figure 2.

The NMR data reported in literature are, apart from some minor differences due to different nomenclature, in agreement with those reported here.[3,8,9,43,44]

The mass spectrometric data are in line with those reported by others.[3,7,9] Typical fragments indicating losses of water and subsequently of a methyl (*iso*-methyl-branch) respectively an ethyl group (*anteiso*-methyl-branch) as reported by Tajima *et al.* for methyl-branched aldehydes of C_9 to C_{11},[45] were detected for the two C_{12} isomers only. The aldehydes of higher

masses underwent stronger fragmentation. Retention indices reported in the literature, if available, are in accordance with the results reported here (table 2), and deviations between the determined and theoretical accurate masses were < 5 ppm.

Transformations on semi-preparative scale were conducted by use of the purified *Csα*-DOX. Nevertheless, in contrast to other aldehyde forming enzymes like CARs, *α*-DOXs could be readily applied in whole cell catalysis in future studies.[16,34]

Sensory evaluation of methyl-branched aldehydes.

All methyl-branched aldehydes exhibited green-soapy (coriander leaf-like) and sweety odors with savory-tallowy notes up to C_{14} isomers. The shorter aldehydes had also citrus-like, woody, and herbaceous nuances turning into more metallic, peppery, and waxy qualities with increasing chain-length (table 2). Odors perceived at the ODP were mainly in accordance with the attributes obtained by sniffing at the pure substances. However, the latter method enabled a more precise description of special nuances by avoiding rather general descriptors. Nevertheless, an interference with olfactory active impurities cannot completely be ruled out, despite there were only in a few cases traces with weak olfactory detectability found by GC–FID–O-analysis. The odor qualities of some of the investigated representatives were characterized for the first time in detail in this study. As no chiral analyses were performed, potentially differing odor qualities of enantiomers of the *anteiso*-aldehydes could not be evaluated.

The role of 12-methyltridecanal as a character impact compound of stewed beef is well-known,[3,4,46] while much less is known on the other aldehydes. According to the literature, 10-methylundecanal showed a sweety, citrus-, and peel-like odor,[47] which is in line with our results. Werkhoff *et al.* reported the occurrence of the C_{13}–C_{15}-aldehydes in beef.[7] They

detected retro-nasal flavor impressions, which greatly depended on the composition of the aqueous medium used (table 2). *Iso*- (C_{12}–C_{16}) as well as *anteiso*- (C_{11}, C_{13}, and C_{15}) fatty aldehydes were additionally detected in Gouda cheese, where they seem to be responsible for the characteristic flavor developing during the ripening. The same authors discussed a change from citrus- to beef-like odors of the aldehydes with increasing chain lengths.[8,9]

Odor thresholds of *iso*- and *anteiso*-fatty aldehydes are known to be comparatively low,[45,48] especially those of the C_{13} and C_{14} isomers.[3,9] Our results (0.18–70 ng/L air, cf. Supporting Information S7) are largely in agreement with the literature. However, compared to the literature, a nearly fivefold lower threshold was observed for 11-methyltridecanal which highlights it, together with its *iso*-isomer, as the most potent of this class. As already stated above, no chiral analyses were carried out. Data concerning the enantiomeric ratios of the *anteiso*-aldehydes were not obtained, which could probably influence the resulting threshold values.

Due to their pleasant odor qualities in combination with low odor thresholds, *iso*- and *anteiso*-fatty aldehydes represent promising candidates for applications in flavorings. Some of them have been approved in the European Union as flavorings. According to evaluations of the European Food Safety Authority, there is no safety concern at the estimated levels of intake.[49,50] An auspicious and sustainable approach for the biotechnological production of these substances was demonstrated. Up-scaling of the process as well as identification of natural sources of the branched-chain fatty acid substrates will be subject of a future study.

Abbreviations used

445 *α*-DOX, *α*-dioxygenase; CAR, carboxylic acid reductase; CBB, Coomassie Brilliant Blue;
446 *Csα*-DOX, *α*-dioxygenase originating from *Crocosphaera subtropica*; DVB, divinylbenzene;
447 IPTG, isopropyl-*β*-D-thiogalactopyranoside; LB, Luria-Bertani; Ni-NTA, nickel-nitrilotriacetic
448 acid agarose; O, olfactometry/olfactometric; ODP, olfactory detection port; *Osα*-DOX,
449 *α*-dioxygenase originating from *Oryza sativa*; PDMS, polydimethylsiloxane; RI, retention index;
450 SPME, solid phase microextraction; TBST, tris-buffered saline with Tween® 20; TMS,
451 tetramethylsilane; TRIS, tris(hydroxymethyl)-aminomethane

452

453 Acknowledgement

454 The authors are grateful to Symrise AG (Holzminden, Germany) for providing methyl-
455 branched fatty acids as substrates. Special thanks go to the following colleagues for their
456 support: K. D. Bakonyi, F. Birk, F. Buerger, M. Gand, J. C. Guder, A. Hannappel, C. Mewe, H.
457 Schewe, and A. Spielmeyer.

458

459

460 Supporting information description

461 S1: Western blot of His-tagged *Csα*-DOX

462 S2: Alignment of the putative *Csα*-DOX and three plant *α*-DOX sequences

463 S3: Phylogenetic tree of Csα-DOX and established plant α-DOX enzymes

464 S4: Substrate screening of *Osα*-DOX

465 S5: Influence of C-terminal His-tag on *Csα*-DOX activity

466 S6: Michaelis-Menten kinetics of *Csα*-DOX for myristic and 13-methyltetradecanoic acid

467 S7: Odor thresholds of unbranched, *iso*-, and *anteiso*-methyl-branched aldehydes

468 S8: GC-MS, HRMS and NMR spectra of 11- and 12-methyltridecanal

This material is available free of charge via the Internet at http://pubs.acs.org.

Notes

The authors declare no competing financial interest.

References

(1) Surburg, H.; Panten, J. *Common fragrance and flavor materials: Preparation, properties and uses*, 5th ed.; Wiley-VCH: Weinheim, Germany, 2006.

(2) Burdock, G. A.; Fenaroli, G. *Fenaroli's Handbook of Flavor Ingredients*, 6th ed.; CRC: Boca Raton, FL, 2010.

(3) Guth, H.; Grosch, W. 12-Methyltridecanal, a Species-Specific Odorant of Stewed Beef. *Lebensm.-Wiss. Technol.* **1993**, *26*, 171–177.

(4) Guth, H.; Grosch, W. Identification of the Character Impact Odorants of Stewed Beef Juice by Instrumental Analyses and Sensory Studies. *J. Agric. Food Chem.* **1994**, *42*, 2862–2866.

(5) Haro-Guzmán, L. Composition of Distilled Oils. In *Citrus Oils: Composition, Advanced Analytical Techniques, Contaminants, and Biological Activity*; Dugo, G., Mondello, L., Eds.; CRC: Boca Raton, FL, 2010; pp 193–218.

(6) Steinhaus, M. Characterization of the Major Odor-Active Compounds in the Leaves of the Curry Tree *Bergera koenigii* L. by Aroma Extract Dilution Analysis. *J. Agric. Food Chem.* **2015**, *63*, 4060–4067.

(7) Werkhoff, P.; Brüning, J.; Emberger, R.; Güntert, M.; Hopp, R. Flavor Chemistry of Meat Volatiles: New Results on Flavour Components from Beef, Pork, and Chicken. In *Recent Developments in Flavor and Fragrance Chemistry: Proceedings of the 3rd International*

Haarmann & Reimer Symposium; Hopp, R., Mori, K., Eds.; Wiley-VCH: Weinheim, Germany, 1993; pp 183–213.

(8) Inagaki, S.; Fujikawa, S.; Wada, Y.; Kumazawa, K. Identification of the possible new odor-active compounds "12-methyltridecanal and its analogs" responsible for the characteristic aroma of ripe Gouda-type cheese. *Biosci., Biotechnol., Biochem.* **2015**, *79*, 2050–2056.

(9) Inagaki, S.; Fujikawa, S.; Wada, Y.; Kumazawa, K. Characterization of Methyl-Branched Aldehyde Analogs as Potent Odorants in Ripe Natural Cheeses (in Japanese). *Nippon Shokuhin Kagaku Kogaku Kaishi* **2016**, *63*, 388–393.

(10) Kaneda, T. Iso- and Anteiso-Fatty Acids in Bacteria: Biosynthesis, Function, and Taxonomix Significance. *Microbiological Reviews* **1991**, *55*, 288–302.

(11) Kerscher, R.; Nürnberg, K.; Voigt, J.; Schieberle, P.; Grosch, W. Occurrence of 12-methyltridecanal in microorganisms and physiological samples isolated from beef. *J. Agric. Food Chem.* **2000**, *48*, 2387–2390.

(12) Fraatz, M. A.; Goldmann, M.; Geissler, T.; Gross, E.; Backes, M.; Hilmer, J.-M.; Ley, J.; Rost, J.; Francke, A.; Zorn, H. Biotechnological Production of Methyl-Branched Aldehydes. *J. Agric. Food Chem.* **2018**, *66*, 2387–2392.

(13) Derrington, S. R.; Turner, N. J.; France, S. P. Carboxylic acid reductases (CARs): An industrial perspective. *J. Biotechnol.* **2019**, *304*, 78–88.

(14) Winkler, M. Carboxylic acid reductase enzymes (CARs). *Curr. Opin. Chem. Biol.* **2018**, *43*, 23–29.

(15) Kunjapur, A. M.; Tarasova, Y.; Prather, K. L. J. Synthesis and Accumulation of Aromatic Aldehydes in an Engineered Strain of *Escherichia coli*. *J. Am. Chem. Soc.* **2014**, *136*, 11644–11654.

(16) Maurer, S.; Schewe, H.; Schrader, J.; Buchhaupt, M. Investigation of fatty aldehyde and alcohol synthesis from fatty acids by αDox- or CAR-expressing *Escherichia coli*. *J. Biotechnol.* **2019**, *305*, 11–17.

(17) Goulah, C. C.; Zhu, G.; Koszelak-Rosenblum, M.; Malkowski, M. G. The Crystal Structure of *α*-Dioxygenase Provides Insight into Diversity in the Cyclooxygenase-Peroxidase Superfamily. *Biochemistry* **2013**, *52*, 1364–1372.

(18) Koszelak-Rosenblum, M.; Krol, A. C.; Simmons, D. M.; Goulah, C. C.; Wroblewski, L.; Malkowski, M. G. His-311 and Arg-559 Are Key Residues Involved in Fatty Acid Oxygenation in Pathogen-Inducible Oxygenase. *J. Biol. Chem.* **2008**, *283*, 24962–24971.

(19) Hamberg, M.; Ponce de Leon, I.; Rodriguez, M. J.; Castresana, C. *α*-dioxygenases. *Biochem. Biophys. Res. Commun.* **2005**, *338*, 169–174.

(20) Stumpf, P. K. Fat Metabolism in Higher Plants: VIII. Saturated Long Chain Fatty Acid Peroxidase. *J. Biol. Chem.* **1956**, 643–649.

(21) Shine, W. E.; Stumpf, P. K. Far Metabolism in Higher Plants. Recent Studies on Plant *α*-Oxidation Systems. *Arch. Biochem. Biophys.* **1974**, *162*, 147–157.

(22) Galliard, T.; Matthew, J. A. The enzymatic formation of long chain aldehydes and alcohols by *α*-oxidation of fatty acids in extracts of cucumber fruit (*Cucumis sativus*). *Biochim. Biophys. Acta* **1976**, *424*, 26–35.

(23) Hitchcock, C.; James, A. T. The Mechanism of *α*-Oxidation in Leaves. *Biochim. Biophys. Acta* **1966**, 413–424.

(24) Mareš, J.; Johansen, J. R.; Hauer, T.; Zima, J.; Ventura, S.; Cuzman, O.; Tiribilli, B.; Kaštovský, J. Taxonomic resolution of the genus *Cyanothece* (Chroococcales, Cyanobacteria), with a treatment on *Gloeothece* and three new genera, *Crocosphaera*, *Rippkaea*, and *Zehria*. *J. Phycol.* **2019**, *55*, 578–610.

(25) Li, C.; Wen, A.; Shen, B.; Lu, J.; Huang, Y.; Chang, Y. FastCloning: a highly simplified, purification-free, sequence- and ligation-independent PCR cloning method. *BMC biotechnol.* **2011**, *11*, 92.

(26) Laemmli, U. K. Cleavage of Structural Proteins during the Assembly of the Head of Bacteriophage T4. *Nature* **1970**, *227*, 680–685.

(27) Towbin, H.; Staehelin, T.; Gordon, J. Electrophoretic transfer of proteins from polyacrylamide gels to nitrocellulose sheets: Precedure and some applications. *Proc. Natl. Acad. Sci. U. S. A.* **1979**, *76*, 4350–4354.

(28) Smith, P. K.; Krohn, R. I.; Hermanson, G. T.; Mallia, A. K.; Gartner, F. H.; Provenzano, M. D.; Fujimoto, E. K.; Goeke, N. M.; Olson, B. J.; Klenk, D. C. Measurement of Protein Using Bicinchoninic Acid. *Anal. Biochem.* **1985**, *150*, 76–85.

(29) Gasteiger, E.; Hoogland, C.; Gattiker, A.; Duvaud, S.; Wilkins, M. R.; Appel, R. D.; Bairoch, A. Protein Identification and Analysis Tools on the ExPASy Server. In *The Proteomics Protocols Handbook*; Walker, J. M., Ed.; Humana Press: Totowa, NJ, 2005; pp 571–607.

(30) Juo, C.-G.; Chen, C.-L.; Lin, S.-T.; Fu, S.-H.; Chen, Y.-T.; Chang, Y.-S.; Yu, J.-S. Mass accuracy improvement of reversed-phase liquid chromatography/electrospray ionization mass spectrometry based urinary metabolomic analysis by post-run calibration using sodium formate cluster ions. *Rapid Commun. Mass Spectrom.* **2014**, *28*, 1813–1820.

(31) Sanz, A.; Moreno, J. I.; Castresana, C. PIOX, a New Pathogen-Induced Oxygenase with Homology to Animal Cyclooxygenase. *Plant Cell* **1998**, *10*, 1523–1537.

(32) Saffert, A.; Hartmann-Schreier, J.; Schön, A.; Schreier, P. A Dual Function α-Dioxygenase-Peroxidase and NAD^+ Oxidoreductase Active Enzyme from Germinating Pea Rationalizing α-Oxidation of Fatty Acids in Plants. *Plant Physiol.* **2000**, *123*, 1545–1551.

562 (33) Koeduka, T.; Matsui, K.; Akakabe, Y.; Kajiwara, T. Catalytic Properties of Rice α-
563 Oxygenase. A Comparison with Mammalian Prostaglandin H Synthases. *J. Biol. Chem.* **2002**,
564 *277*, 22648–22655.
565 (34) Kaehne, F.; Buchhaupt, M.; Schrader, J. A recombinant α-dioxygenase from rice to
566 produce fatty aldehydes using *E. coli*. *Appl. Microbiol. Biotechnol.* **2011**, *90*, 989–995.
567 (35) Boivin, S.; Kozak, S.; Meijers, R. Optimization of protein purification and characterization
568 using Thermofluor screens. *Protein Expression Purif.* **2013**, *91*, 192–206.
569 (36) Hamberg, M.; Sanz, A.; Castresana, C. α-Oxidation of Fatty Acids in Higher Plants. *J. Biol.*
570 *Chem.* **1999**, *274*, 24503–24513.
571 (37) Liu, W.; Wang, L.-H.; Fabian, P.; Hayashi, Y.; McGinley, C. M.; van der Donk, W. A.;
572 Kulmacz, R. J. *Arabidopsis thaliana* fatty acid alpha-dioxygenase-1: evaluation of substrates,
573 inhibitors and amino-terminal function. *Plant Physiol. Biochem.* **2006**, *44*, 284–293.
574 (38) Borge, G. I. A.; Slinde, E.; Nilsson, A. Long-chain saturated fatty acids can be α-oxidised
575 by a purified enzyme (M_r 240 000) in cucumber (*Cucumis sativus*). *Biochim. Biophys. Acta*
576 **1997**, *1344*, 47–58.
577 (39) Zorn, H.; Schüler, M.; Berger, R. G. Pyruvate Decarboxylase Catalysed Formation of
578 Terpenoid α-hydroxy Ketones. *Biocatal. Biotransform.* **2003**, *21*, 341–347.
579 (40) Akakabe, Y.; Matsui, K.; Kajiwara, T. Enantioselective α-Hydroperoxylation of Long-Chain
580 Fatty Acids with Crude Enzyme of Marine Green Alga *Ulva pertusa*. *Tetrahedron Lett.* **1999**,
581 *40*, 1137–1140.
582 (41) Liu, W.; Rogge, C. E.; Bambai, B.; Palmer, G.; Tsai, A.-L.; Kulmacz, R. J. Characterization of
583 the Heme Environment in *Arabidopsis thaliana F*atty Acid α-Dioxygenase-1. *J. Biol. Chem.*
584 **2004**, *279*, 29805–29815.

585 (42) Zhu, G.; Koszelak-Rosenblum, M.; Malkowski, M. G. Crystal structures of α-dioxygenase
586 from *Oryza sativa*: insights into substrate binding and activation by hydrogen peroxide.
587 *Protein Sci.* **2013**, *22*, 1432–1438.
588 (43) Yuasa, Y.; Tsuruta, H. Convenient syntheses of iso-methyl-branched long-chain aliphatic
589 aldehydes, known to contribute significantly to meat flavour. *Flavour Fragrance J.* **2004**, *19*,
590 199–204.
591 (44) Inagaki, S.; Suzuki, H.; Shimizu, Y.; Sekiguchi, M.; Usuki, M.; Fujikawa, S.; Wada, Y.;
592 Kumasawa, K. Taste-improving agent, flavor composition containing it, and method for
593 improving taste of oil/fat-containing food by using it. Japanese patent 2016047011, Apr 7,
594 2016.
595 (45) Tajima, K.; Tanaka, S.; Yamaguchi, T.; Fujita, M. Analysis of Green and Yellow Yuzu Peel
596 Oils (*Citrus junos Tanaka*). Novel Aldehyde Components with Remarkably Low Odor
597 Thresholds. *J. Agric. Food Chem.* **1990**, *38*, 1544–1548.
598 (46) Christlbauer, M.; Schieberle, P. Characterization of the key aroma compounds in beef
599 and pork vegetable gravies á la chef by application of the aroma extract dilution analysis.
600 *Journal of agricultural and food chemistry* **2009**, *57*, 9114–9122.
601 (47) Saito, S.; Takaoka, H.; Kimura, K.; Samuta, Y. Preparation of 5-methylundecanal and 6-
602 methylundecanal and fragrant compositions containing the branched aldehydes and 10-
603 methylundecanal. Japanese patent 2014210751, Nov 13, 2014.
604 (48) Widder, S.; Eggers, M.; Pickenhagen, W. New flavour compounds from orange essence
605 oil. In *Flavour research at the dawn of the twenty-first century: Proceedings of the 10th*
606 *Weurman Flavour Research Symposium*; Le Quéré, J.-L., Ed.; Ed. Tec & Doc: Londres, NY, 2003;
607 pp 745–748.

(49) EFSA Panel on Food Contact Materials, Enzymes, Flavourings and Processing Aids. Scientific Opinion on Flavouring Group Evaluation 01, Revision 2 (FGE.01Rev2): Branched-chain aliphatic saturated aldehydes, carboxylic acids and related esters of primary alcohols and branched-chain carboxylic acids from chemical groups 1 and 2. *EFSA Journal* **2010**, *8*, 1843.

(50) EFSA Panel on Food Contact Materials, Enzymes, Flavourings and Processing Aids. Scientific Opinion on Flavouring Group Evaluation 72, Revision 1 (FGE.72Rev1): Consideration of aliphatic, branched-chain saturated and unsaturated alcohols, aldehydes, acids, and related esters evaluated by the JECFA (61st meeting) structurally related to branched- and straight-chain unsaturated carboxylic acids, esters of these and straight-chain aliphatic saturated alcohols evaluated by EFSA in FGE.05Rev2. *EFSA Journal* **2013**, *11*, 3392.

(51) van den Dool, H.; Kratz, P. D. A Generalization of the Retention Index System Including Linear Temperature Programmed Gas-Liquid Partition Chromatography. *J. Chromatogr. A* **1963**, *11*, 463–471.

Funding sources

Parts of the study have been funded by the German Ministry of Environment, Nature Conservation and Nuclear Safety via the Fachagentur Nachwachsende Rohstoffe (FNR, funding code: 22001617). Financial support by LOEWE – Landes-Offensive zur Entwicklung Wissenschaftlich-oekonomischer Exzellenz-AromaPlus (State Offensive for the Development of Scientific and Economic Excellence) is gratefully acknowledged.

Figure captions

Figure 1: Mechanism of *α*-oxidation of fatty acids according to Hamberg *et al*.[19]

Figure 2: Biotransformation of *iso*- (1) and *anteiso*- (2) methyl-branched fatty acids to their corresponding aldehydes.

Figure 3: SDS–PAGE of *Csα*-DOX (calculated mass 69.9 kDa) preparation after heterologous expression and purification. Lanes 1 and 6 show molecular mass markers, lanes 2–4 cell pellets of BL21(DE3)+pET-28a (blank), BL21(DE3)+pET-28a-*Csα*-DOX, and BL21(DE3)+pET-28a-*Csα*-DOX_C-His (variant with C-terminal His-tag). Lane 5 shows the purified *Csα*-DOX with C-terminal His-tag.

Figure 4: Activities of crude protein extracts of *Csα*-DOX for oxidation of a homologous series of saturated fatty acids. Error bars indicate standard errors from three biological replicates.

Tables

Table 1: Enzyme kinetic parameters of purified *Csα*-DOX, determined by means of oxygen depletion assay

kinetic parameter[a]	myristic acid	13-methyltetradecanoic acid
Michaelis constant K_m [µM]	26.3 ± 5.6	16.2 ± 2.9
maximum reaction speed v_{max} [U/mg]	3.47 ± 0.45	2.70 ± 0.16
catalytic constant k_{cat} [1/s]	4.03 ± 0.52	3.14 ± 0.19
catalytic efficiency k_{cat}/K_m [1/µM per s]	0.17 ± 0.06	0.20 ± 0.03

[a] Calculated with OriginPro version 2020. Values represent means of biological triplicates. Errors are given as standard errors.

Table 2: Retention indices and odor impressions of the generated methyl-branched aldehydes

Compound	retention indices[a]		odor impressions		flavor impressions (literature)
	polar VF-WAXms	nonpolar DB-5MS	olfactory detection port	pure substance	
9-methyl-undecanal	1674	1380	citrus-like, coriander leaf-like, green, herbaceous, metallic, savory, soapy, waxy, woody	green, hay-like, herbaceous, soapy, savory, woody	
10-methyl-undecanal	1660 (1662)	1373 (1350)	citrus-like, coriander leaf-like, creamy, fatty, green, herbaceous, soapy, sweety	citrus-like, creamy, green, herbaceous, soapy	
10-methyl-dodecanal	1780 (1781)	1482 (1482)	creamy, coriander leaf-like, green, herbaceous,	savory, sweety, tallowy, wasabi-like, woody	aldehyde-like, fatty, tallowy[b] flowery, orange-like[c]

			metallic, savory, soapy, tallowy, waxy		
11-methyl-dodecanal	1766 (1767)	1476 (1452)	citrus-like, coriander leaf-like, green, herbaceous, metallic, savory, soapy, sweety, waxy	herbaceous, savory, soapy	aldehyde-like, cooked meat-like, fatty, tallowy[b]
11-methyl-tridecanal	1886	1584	coriander leaf-like, green, herbaceous, metallic, soapy, sweety, tallowy, waxy	savory, sweety, tallowy, wasabi-like	
12-methyl-tridecanal	1871 (1872)	1576 (1558)	coriander leaf-like, green, herbaceous, metallic,	green, metallic, peppery, sweety, tallowy	cheese-like, fatty[b] citrus-like, fruity, orange-

			savory, soapy, sweety, tallowy		like, orange peel oil[c]
12-methyl-tetradecanal	1992 (1992)	1686 (1663)	coriander leaf-like, green, metallic, soapy, sweety, waxy	metallic, peppery, sweety	aldehyde-like, cheesy, fatty, peppery, soapy, tallowy, waxy[b] citrus-like, fruity, orange-like, orange peel oil[c]
13-methyl-tetradecanal	1976 (1976)	1678 (1656)	coriander leaf-like, green, metallic, soapy, sweety, waxy	green, metallic, sweety	cooked meat-like, fatty, woody[b] aldehyde-like, sweety, woody[c]

[a] retention indices were calculated according to van den Dool and Kratz;[51] numbers in brackets depict literature data reported by Inagaki *et al.* on polar DB-WAX respective nonpolar DB-1 column,[8] [b] retro-nasal impressions in either salty or [c] sweet aqueous medium according to Werkhoff *et al*.[7]

Figures graphics

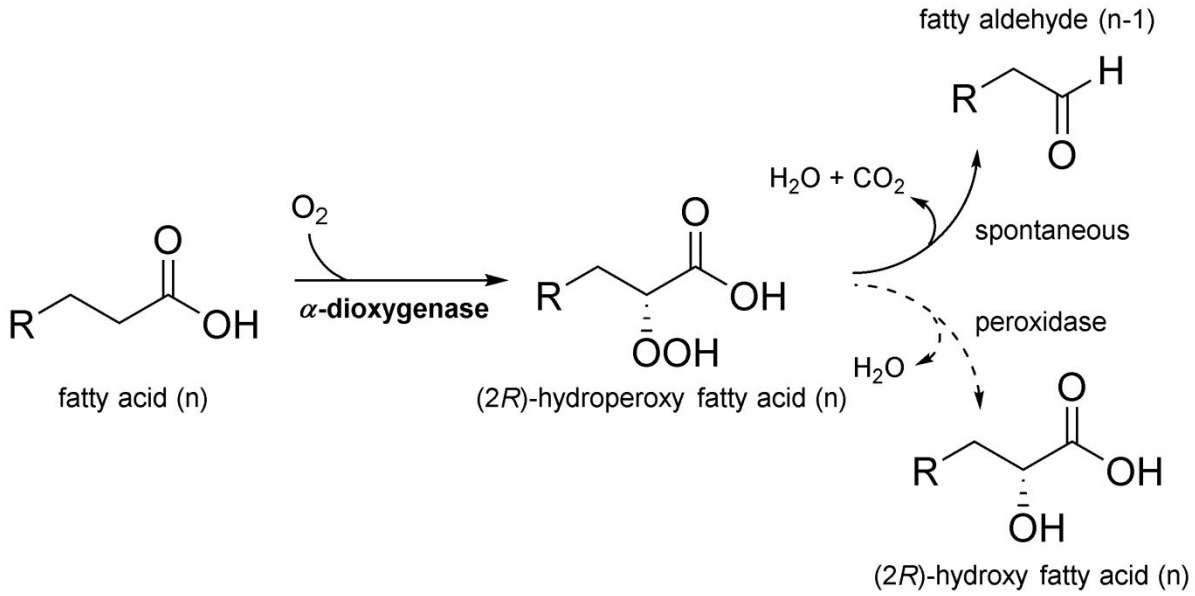

Figure 1

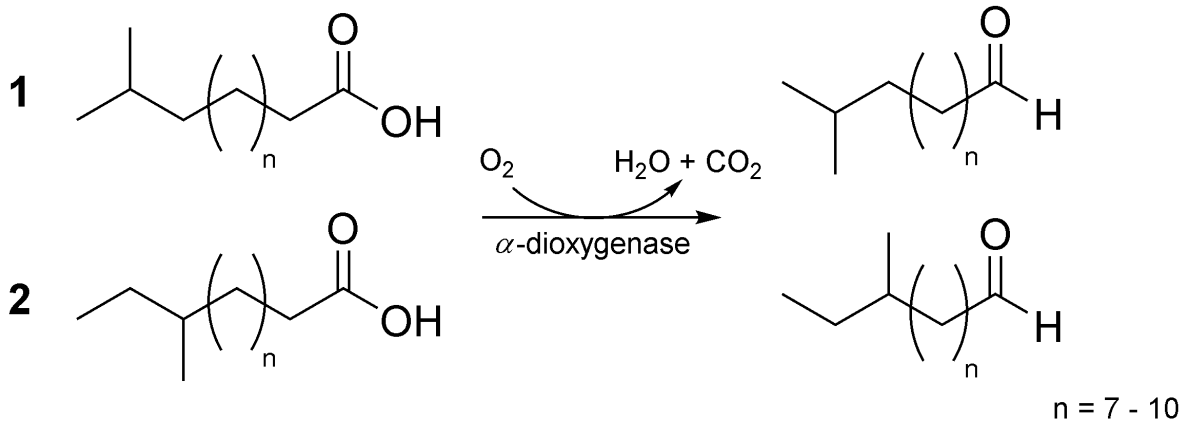

Figure 2

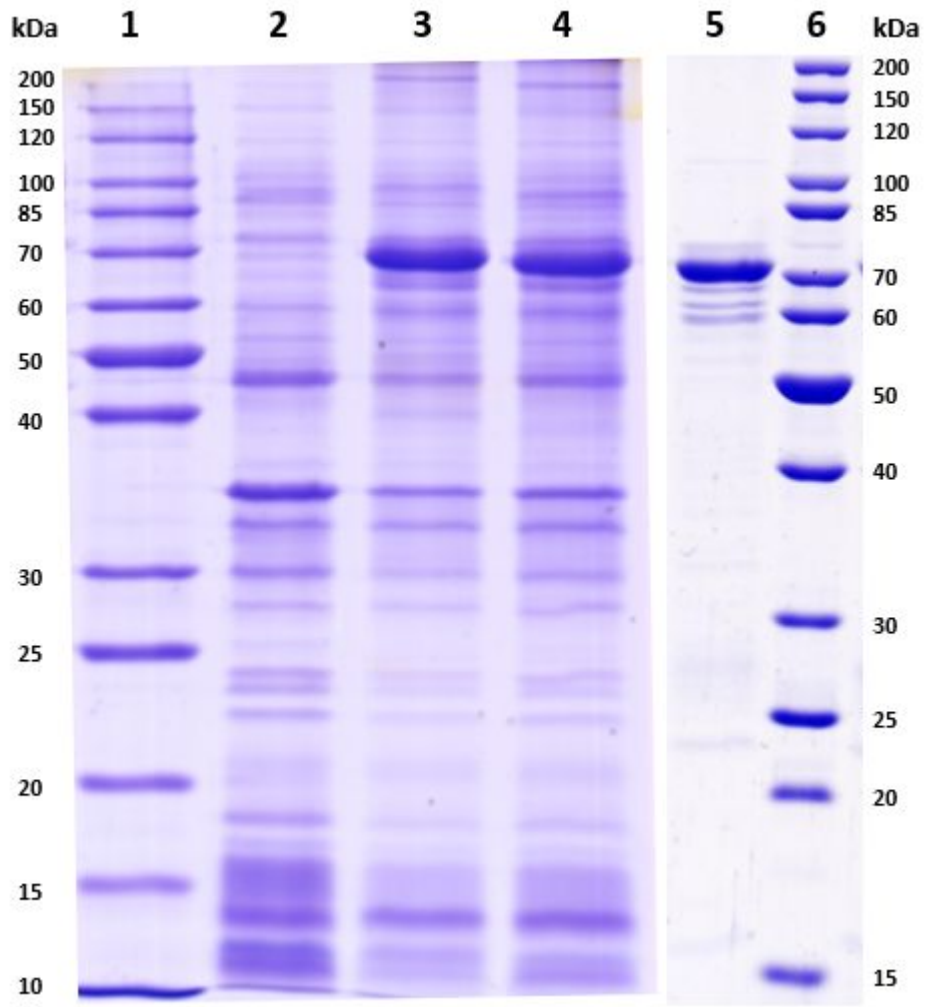
kDa
1
2
3
4
5
6
kDa
200
150
120
100
85
70
60
50
40
30
25
20
15
10
200
150
120
100
85
70
60
50
40
30
25
20
15

Figure 3

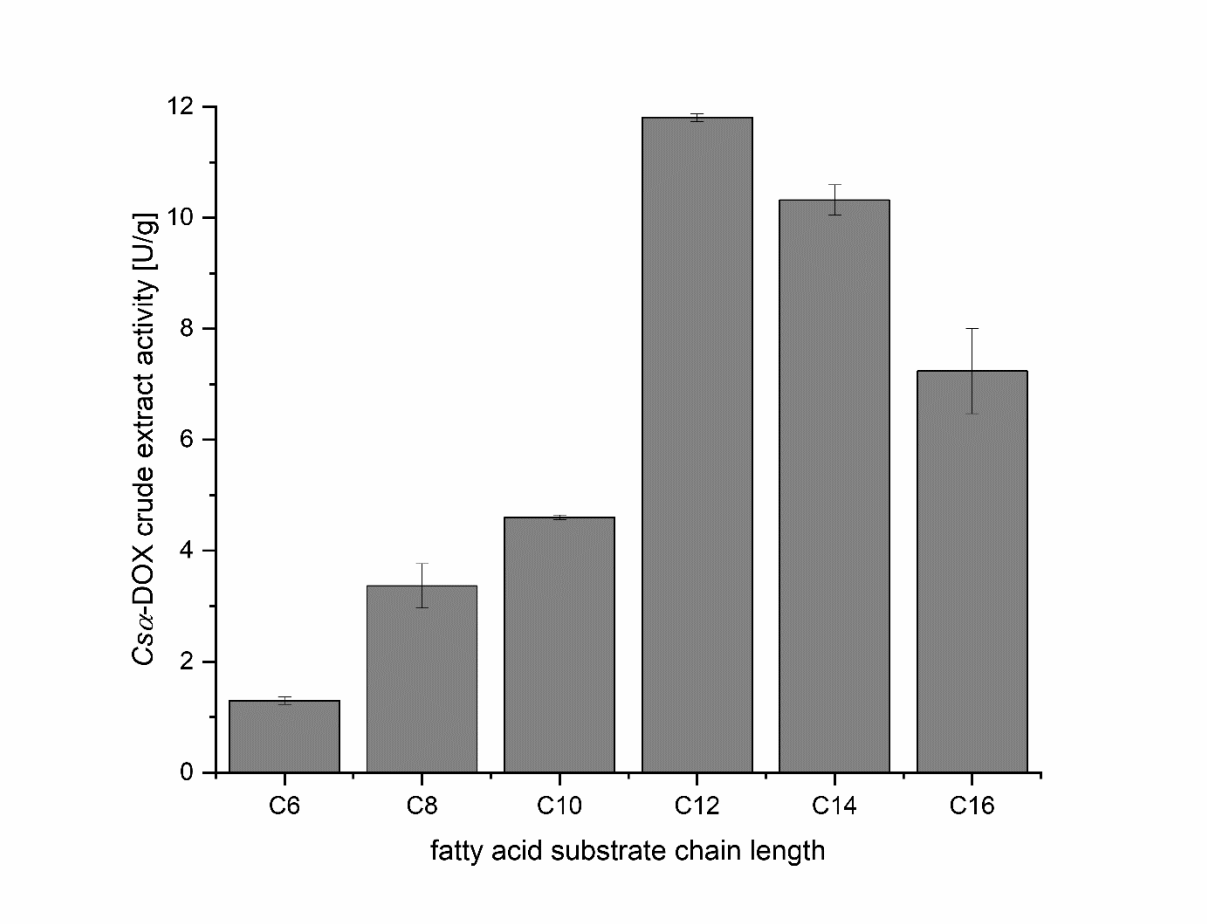
Csα-DOX crude extract activity [U/g]
0
2
4
6
8
10
12
C6
C8
C10
C12
C14
C16
fatty acid substrate chain length

Figure 4

TOC graphic:

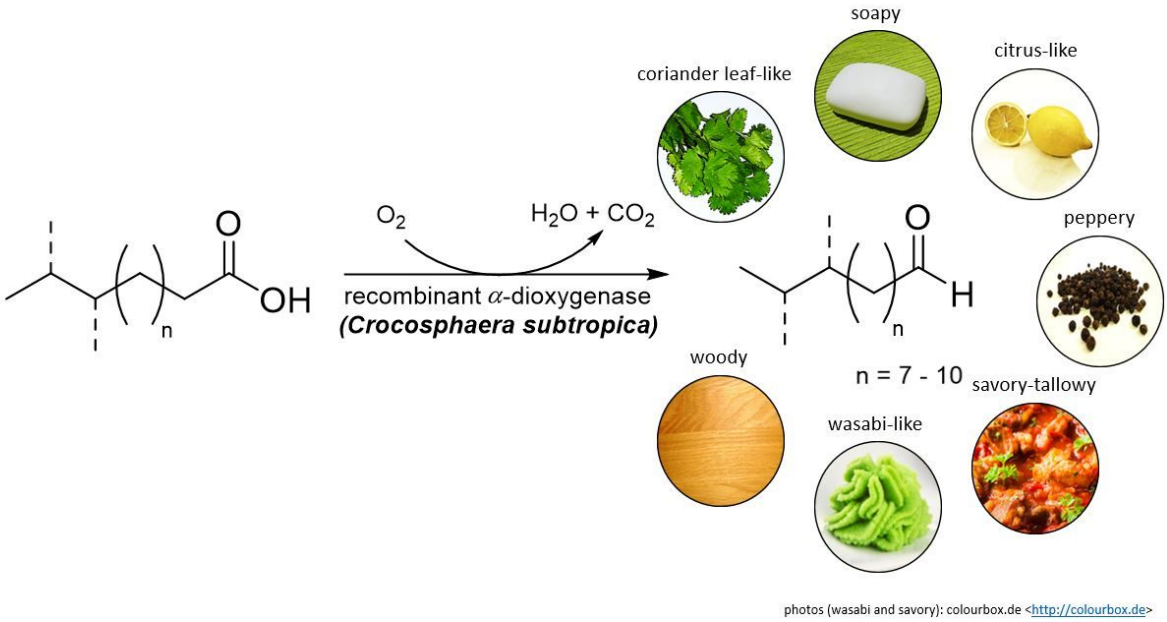
soapy
coriander leaf-like
citrus-like
O
OH
n
O2
H2O + CO2
recombinant α-dioxygenase
(Crocosphaera subtropica)
O
H
n
peppery
woody
n = 7 - 10
savory-tallowy
wasabi-like
photos (wasabi and savory): colourbox.de <http://colourbox.de>